Table 2. Estimated Mean Change from Baseline for the Coprimary and Secondary Outcomes, According to a Mixed-Model Repeated-Measures Analysis.*

Outcome	Placebo	Semagacestat, 100 mg	Semagacestat, 140 mg	P Values	
				Semagacestat, 100 mg, vs. Placebo	Semagacestat, 140 mg, vs. Placebo
ADAS-cog score				0.15	0.07
No. of participants with results	486	483	497		
Mean change in score (95% CI)	6.4 (5.48 to 7.40)	7.5 (6.44 to 8.53)	7.8 (6.72 to 8.85)		
ADCS–ADL†				0.14	<0.001
No. of participants with results	480	481	490		
Mean change in score (95% CI)	−9.0 (−10.37 to −7.67)	−10.5 (−11.94 to −9.07)	−12.6 (−14.1 to −11.2)		
CDR-SB‡				0.06	<0.01
No. of participants with results	485	480	494		
Mean change in score (95% CI)	2.4 (2.06 to 2.67)	2.8 (2.47 to 3.13)	3.1 (2.73 to 3.41)		
NPI§				0.28	0.05
No. of participants with results	473	463	472		
Mean change in score (95% CI)	1.9 (0.69 to 3.12)	2.9 (1.58 to 4.21)	3.7 (2.36 to 5.08)		
MMSE				0.23	0.03
No. of participants with results	400	328	303		
Mean change in score (95% CI)	−3.4 (−3.95 to −2.86)	−3.9 (−4.51 to −3.30)	−4.3 (−4.99 to −3.68)		

* In this mixed-model repeated-measures analysis, the dependent variable was the change from the baseline score at each postbaseline visit during the initial treatment period. Fixed effects included the baseline score, treatment, MMSE score at screening, visit, treatment effect according to visit, concomitant use of an acetylcholinesterase inhibitor (usually donepezil) or memantine at baseline (yes or no), and age at baseline. Study visit was treated as a categorical variable. "Participant" was included in the model as the random effect. An unstructured covariance matrix was used to model the within-participant variance–covariance errors. The primary comparisons of interest were those of 140 mg of semagacestat versus placebo, 100 mg of semagacestat versus placebo, and 140 mg versus 100 mg of semagacestat at week 76. The numbers of participants are based on those who had a baseline score and at least one postbaseline score for each instrument. CI denotes confidence interval.

† For the Alzheimer's Disease Cooperative Study–Activities of Daily Living (ADCS-ADL) scale, the range is 0 to 78, and higher scores indicate better function.

‡ For the Clinical Dementia Rating–Sum of Boxes (CDR-SB), the range is 0 to 18, and higher scores indicate poorer function.

§ For the Neuropsychiatric Inventory (NPI), the range is 0 to 144, and higher scores indicate poorer function.

Donepezil Levels

Plasma donepezil levels decreased by approximately 30% between baseline and week 52 in both semagacestat groups (−20.3±19.2 ng per milliliter in the lower-dose group and −20.4±19.7 ng per milliliter in the higher-dose group, vs. 0.46±18.4 ng per milliliter in the placebo group; P<0.001 for both comparisons). Reductions in donepezil levels did not correlate with worsening of the coprimary or secondary outcomes.

Biologic Markers and Neuroimaging

Among the 1467 participants in whom plasma levels of Aβ were measured at baseline, 844 had levels measured at week 76 or at early termination. In the group receiving 100 mg of semagacestat, there were reductions from baseline in levels of Aβ40 (mean, 38%; median, 47%) and Aβ42 (mean, 5%; median, 9%); in the group receiving 140 mg, there were greater reductions in levels of both Aβ40 (mean, 48%; median, 54%) and Aβ42 (mean, 18%; median, 24%) (P<0.001 by analysis of covariance for all comparisons). There was no significant change from baseline in levels of Aβ40 or Aβ42 in the placebo group.

Levels of Aβ in the CSF were available for 110 participants at baseline and for 47 of these participants at week 76 or early termination. CSF levels of Aβ40 and Aβ42 (measured 24 to 36 hours after the administration of the study drug or placebo) did not change significantly in any group. Levels of tau protein in the CSF were available for 109 participants at baseline and for 47 of these participants at week 76 or early termination. There were no significant changes from baseline in any of the three study groups.

Table 3. Summary of Adverse Events Occurring during the Study Treatment, According to the MedDRA System or Organ Class and Preferred Term.*

Event	Placebo (N=501)	Semagacestat			Total (N=1534)
		100 mg (N=506)	140 mg (N=527)	Combined (N=1033)	
	percent of participants				
System or organ class					
Neoplasms — benign, malignant, or unspecified	5	15	16	15	12
Skin or subcutaneous-tissue disorders	21	45	52	48	39
Preferred term					
Alopecia	0	1	5	3	2
Basal-cell carcinoma	1	3	5	4	3
Decreased appetite	3	7	11	9	7
Epistaxis	1	3	3	3	2
Eyelash discoloration	0	2	5	3	2
Hair-color changes	1	13	19	16	11
Nausea	5	11	12	11	9
Pruritus	2	3	4	3	3
Rash					
Erythematous	2	5	5	5	4
Macular	4	7	8	8	6
Maculopapular	1	3	5	4	3
Papular	1	3	4	4	3
Skin lesion	1	3	3	3	2
Squamous-cell carcinoma of skin	1	6	5	5	4
Syncope	1	3	3	3	3
Vomiting	4	10	9	9	7
Weight decrease	3	5	9	7	6

* The listed adverse events are those with an incidence of at least 2% in any one group and a rate in the combined semagacestat groups that was at least two times as high as the rate in the placebo group. MedDRA denotes *Medical Dictionary for Regulatory Activities*, version 13.1.

Levels of phospho-tau in the CSF increased by 16% in the placebo group and declined in the groups receiving semagacestat, with declines of 8% in the lower-dose group and 4% in the higher-dose group ($P<0.001$ for both comparisons with placebo).

Among the 208 participants for whom volumetric MRI scans were obtained at baseline, the availability of end-point data differed according to imaging outcome, from a low of 120 scans available for entorhinal cortex volume to 208 scans available for hippocampal volume. A few scans showed greater volumetric loss in patients receiving 140 mg of semagacestat than in those receiving placebo, but the results were inconsistent across imaging regions, and baseline measures showed significant imbalances across treatment groups. One patient had vasogenic edema at baseline, but new vasogenic edema was not seen in patients in any of the groups. PET scans were available for 108 participants at baseline and for 59 of these participants at week 76 or early termination. There were no significant differences among the three groups in changes from baseline FDG-PET or ^{18}F-florbetapir–PET measurements.

Reversal of Adverse Events and Clinical Worsening

After the termination of drug dosing, data were available for 58% of participants (290 of 501)

who were randomly assigned to placebo, 44% (223 of 506) who were assigned to 100 mg of semagacestat, and 41% (214 of 527) who were assigned to 140 mg of semagacestat (including participants who completed the initial 76-week period of study treatment and those who were still receiving the study drug when the trial was stopped). At the end of the 32-week safety-extension phase, changes from baseline in ADAS-cog and ADCS-ADL scores were not significantly different across the three groups. There were no longer significant changes from baseline in body weight in the two semagacestat groups. Some (14.5%) of the adverse events that were present at the end of treatment were reduced in severity or reversed by the end of the extension phase. However, the changes from baseline in levels of phosphorus, IgG, and IgA and in white-cell counts were significant, and alkaline phosphatase levels were elevated in the two semagacestat groups.

DISCUSSION

This randomized, double-blind, placebo-controlled trial showed no benefit of the γ-secretase inhibitor semagacestat for the treatment of mild-to-moderate Alzheimer's disease. Indeed, treatment with semagacestat was associated with dose-related clinical worsening on multiple primary and secondary outcome measures, including measures of activities of daily living measure (ADCS-ADL score), global functioning (CDR-SB), secondary cognitive functioning (MMSE), and quality of life (EQ-5D) in the group receiving the higher dose of semagacestat. Although donepezil levels were reduced in both groups receiving semagacestat (levels were probably elevated as a result of CYP3A4 induction), this pharmacologic effect does not explain the clinical worsening.

The study was stopped early after a futility analysis, which was conducted earlier than planned, once clinical worsening and safety concerns were identified. Patients receiving semagacestat had more adverse events and more serious adverse events and were more likely to discontinue the study because of adverse events than patients receiving placebo. There were also more gastrointestinal symptoms, infections, and nonmelanoma skin cancers in the semagacestat groups. Changes from baseline laboratory values that were associated with the drug included reductions in IgG and IgA levels and alterations of immune-cell populations (reduced levels of CD19 lymphocytes, reduced levels of monocytes, and eosinophilia). Findings consistent with a drug-induced Fanconi's syndrome were also detected. At the end of the 32-week extension phase of the study, many of the renal and immunologic alterations associated with treatment had not fully resolved.

These disappointing results call for careful further analysis of the data in order to learn as much as possible about the reasons for the clinical worsening. Since Notch and other proteins are also substrates for γ-secretase,[1-4] the inhibition of γ-secretase can interfere with Notch receptor–related nuclear signaling and with the function of cell-surface receptors and the proteins involved in embryonic development, hematopoiesis, cell adhesion, and other cell–cell contacts. A recent report suggests that most, if not all, such inhibitors also inhibit Notch, and that semagacestat may be more selective for Notch than for APP processing by γ-secretase.[23] Since the adverse-event profile of the drug included alterations of immune cells, gastrointestinal symptoms, skin reactions, and skin cancers, it is plausible that the inhibition of Notch accounted for many of these adverse events. The question that is more difficult to answer is whether interference with Notch, or some other receptor or protein in the brain, accounted for the clinical worsening seen in the groups receiving semagacestat.

Alternatively, the clinical worsening may have been related to the effects of semagacestat on its target — APP metabolism by the γ-secretase complex. There is evidence from the data on biologic markers that this target was engaged — specifically, there were reductions in plasma levels of Aβ40 and Aβ42. However, the lack of significant reductions in CSF levels of these Aβ proteins at the time point selected for assessment suggests that the target was engaged peripherally rather than in the brain.[24] The absence of treatment-related changes detected in other brain imaging studies, such as FDG-PET, amyloid imaging with PET, and volumetric MRI studies, could be due to a lack of relevant effects, an insufficient magnitude of effects, imbalances across the subgroups at baseline, or an inadequate sample size or assessment period. However, the absence of between-group differences in these outcomes also suggests that amyloid reduction by semagacestat did not have a directly detrimental effect on the brain.

A notable aspect of the current report is the willingness of the sponsor to provide its proprietary data sets to an independent committee for analysis and publication. An important limitation of the study is that it was halted early, which meant that the number of participants and the duration of their participation were limited. Another, concurrent study of the effect of semagacestat in patients with mild-to-moderate Alzheimer's disease (140 mg vs. placebo) was also terminated early because of the findings reported here.

In conclusion, the γ-secretase inhibitor semagacestat was associated with significant toxic effects that were probably related to its effects on proteins other than APP. The drug was also associated with clinical worsening. The question of whether this worsening represents an on-target effect of central γ-secretase inhibition and central Aβ reduction or an unintended effect related to the known engagement of other inhibitory substrates remains unanswered.

Supported by Eli Lilly and the University of California at San Diego (the latter as a fiduciary for the Alzheimer's Disease Cooperative Study), a clinical-trials consortium established by the National Institute on Aging.

Disclosure forms provided by the authors are available with the full text of this article at NEJM.org.

REFERENCES

1. Jack C, Berezovska O, Wolfe MS, Hyman BT. Effect of PS1 deficiency and an APP gamma-secretase inhibitor on Notch1 signaling in primary mammalian neurons. Brain Res Mol Brain Res 2001;87:166-74.
2. Geling A, Steiner H, Willem M, Bally-Cuif L, Haass C. A gamma-secretase inhibitor blocks Notch signaling in vivo and causes a severe neurogenic phenotype in zebrafish. EMBO Rep 2002;3:688-94.
3. Micchelli CA, Esler WP, Kimberly WT, et al. Gamma-secretase/presenilin inhibitors for Alzheimer's disease phenocopy Notch mutations in Drosophila. FASEB J 2003;17:79-81.
4. Wong GT, Manfra D, Poulet FM, et al. Chronic treatment with gamma-secretase inhibitor LY-411,575 inhibits beta-amyloid peptide production and alters lymphopoiesis and intestinal cell differentiation. J Biol Chem 2004;279:12876-82.
5. May PC, Yang Z, Li W-Y, Hyslop PA, Siemers E, Boggs LN. Multi-compartmental pharmacodynamic assessment of the functional gamma-secretase inhibitor LY450139 dihydrate in PDAPP transgenic mice and non-transgenic mice. Neurobiol Aging 2004;25:Suppl 2:S65.
6. Evin G, Semee MF, Masters CL. Inhibition of γ-secretase as a therapeutic intervention for Alzheimer's disease: prospects, limitations and strategies. CNS Drugs 2006;20:351-72.
7. Siemers ER, Quinn JF, Kaye J, et al. Effects of a gamma-secretase inhibitor in a randomized study of patients with Alzheimer's disease. Neurology 2006;66:602-4.
8. Bateman RJ, Siemers ER, Mawuenyega KG, et al. A γ-secretase inhibitor decreases amyloid-β production in the central nervous system. Ann Neurol 2009;66:48-54.
9. Gitter BD, Czilli DL, Li W, et al. Stereoselective inhibition of amyloid beta peptide secretion by LY450139, a novel functional gamma-secretase inhibitor. Neurobiol Aging 2004;25:Suppl 2:S571.
10. Siemers E, Skinner M, Dean RA, et al. Safety, tolerability and changes in amyloid beta concentrations after administrations of a gamma-secretase inhibitor in volunteers. Clin Neuropharmacol 2005;28:126-32.
11. Fleisher AS, Raman R, Siemers ER, et al. Phase 2 safety trial targeting amyloid beta production with a gamma-secretase inhibitor in Alzheimer disease. Arch Neurol 2008;65:1031-8.
12. Sheikh JL, Yesavage JA. Geriatric Depression Scale (GDS): recent evidence and development of the shorter version. In: Brink TL, ed. Clinical gerontology: a guide to assessment and intervention. New York: Haworth Press, 1986:165-74.
13. Folstein MF, Folstein SE, McHugh PR. "Mini-mental state": a practical method for grading the cognitive state of patients for the clinician. J Psychiatr Res 1975;12:189-98.
14. McKhann G, Drachman D, Folstein M, Katzman R, Price D, Stadlan EM. Clinical diagnosis of Alzheimer's disease: report of the NINCDS-ADRDA Work Group under the auspices of Department of Health and Human Services Task Force on Alzheimer's disease. Neurology 1984;34:939-44.
15. Mohs RC, Knopman D, Petersen RC, et al. Development of cognitive instruments for use in clinical trials of antidementia drugs: additions to the Alzheimer's Disease Assessment Scale that broaden its scope. Alzheimer Dis Assoc Disord 1997;11:Suppl 2:S13-S21.
16. Galasko D, Bennett D, Sano M, et al. An inventory to assess activities of daily living for clinical trials in Alzheimer's disease. Alzheimer Dis Assoc Disord 1997;11:Suppl 2:S33-S39.
17. Berg L, Miller JP, Baty J, Rubin EH, Morris JC, Figiel G. Mild senile dementia of the Alzheimer's type: 4. Evaluation of intervention. Ann Neurol 1992;31:242-9.
18. O'Bryant SE, Waring SC, Cullum CM, et al. Staging dementia using Clinical Dementia Rating Scale Sum of Box scores: a Texas Alzheimer's Research Consortium study. Arch Neurol 2008;65:1091-5.
19. Cummings JL, Mega M, Gray K, Rosenberg-Thompson S, Carusi DA, Gornbein J. The Neuropsychiatric Inventory: comprehensive assessment of psychopathology in dementia. Neurology 1994;44:2308-14.
20. Wimo A, Wetterholm A-L, Mastey V, Winbald B. Evaluation of the healthcare resource utilization and caregiver time in anti-dementia drug trials. In: Wimo A, Jönsson B, Karlsson G, Winblad B, eds. The health economics of dementia. London: Wiley, 1998:465-99.
21. Kind P. The EuroQol instrument: an index of health-related quality of life. In: Spilker B, ed. Quality of life and pharmacoeconomics in clinical trials. 2nd ed. Philadelphia: Lippincott-Raven, 1996:191-201.
22. Wallace JI, Schwartz RS, LaCroix AZ, Uhlmann RF, Pearlman RA. Involuntary weight loss in older outpatients: incidence and clinical significance. J Am Geriatr Soc 1995;43:329-37.
23. Chávez-Gutiérrez L, Bammens L, Benilova I, et al. The mechanism of γ-secretase dysfunction in familial Alzheimer disease. EMBO J 2012;31:2261-74.
24. Roher AE, Esh CL, Kokjohn TA, et al. Aβ peptides in human plasma and tissues and their significance for Alzheimer's disease. Alzheimers Dement 2009;5:18-29.

Neuroradiology (2013) 55:869–875
DOI 10.1007/s00234-013-1193-2

DIAGNOSTIC NEURORADIOLOGY

Diffeomorphic Anatomical Registration Through Exponentiated Lie Algebra provides reduced effect of scanner for cortex volumetry with atlas-based method in healthy subjects

Masami Goto · Osamu Abe · Shigeki Aoki · Naoto Hayashi · Tosiaki Miyati · Hidemasa Takao · Takeshi Iwatsubo · Fumio Yamashita · Hiroshi Matsuda · Harushi Mori · Akira Kunimatsu · Kenji Ino · Keiichi Yano · Kuni Ohtomo · Japanese Alzheimer's Disease Neuroimaging Initiative

Received: 18 January 2013 / Accepted: 12 April 2013 / Published online: 26 April 2013

Abstract
Introduction This study aimed to investigate whether the effect of scanner for cortex volumetry with atlas-based method is reduced using Diffeomorphic Anatomical Registration Through Exponentiated Lie Algebra (DARTEL) normalization compared with standard normalization.
Methods Three-dimensional T1-weighted magnetic resonance images (3D-T1WIs) of 21 healthy subjects were obtained and evaluated for effect of scanner in cortex volumetry. 3D-T1WIs of the 21 subjects were obtained with five MRI systems. Imaging of each subject was performed on each of five different MRI scanners. We used the Voxel-Based Morphometry 8 tool implemented in Statistical Parametric Mapping 8 and WFU PickAtlas software (Talairach brain atlas theory). The following software default settings were used as bilateral region-of-interest labels: "Frontal Lobe," "Hippocampus," "Occipital Lobe," "Orbital Gyrus," "Parietal Lobe," "Putamen," and "Temporal Lobe."
Results Effect of scanner for cortex volumetry using the atlas-based method was reduced with DARTEL normalization compared with standard normalization in Frontal Lobe, Occipital Lobe, Orbital Gyrus, Putamen, and Temporal Lobe; was the same in Hippocampus and Parietal Lobe;

M. Goto (✉) · K. Ino · K. Yano
Department of Radiological Technology, University of Tokyo Hospital, 7-3-1 Hongo, Bunkyo-ku, Tokyo 113-8655, Japan
e-mail: car6_pa2_rw@yahoo.co.jp

O. Abe
Department of Radiology, Nihon University School of Medicine, 30-1 Oyaguchi Kami-cho, Itabashi-ku, Tokyo 173-8610, Japan

S. Aoki
Department of Radiology, Juntendo University, 3-1-3 Hongo, Bunkyo-ku, Tokyo 113-8431, Japan

N. Hayashi
Department of Computational Diagnostic Radiology and Preventive Medicine, University of Tokyo Hospital, 7-3-1 Hongo, Bunkyo-ku, Tokyo 113-8655, Japan

T. Miyati
Graduate School of Medical Science, Kanazawa University, Tsunomatyou, Kanazawa 920-1192, Japan

H. Takao · H. Mori · A. Kunimatsu · K. Ohtomo
Department of Radiology and Department of Computational Diagnostic Radiology and Preventive Medicine, University of Tokyo Hospital, 7-3-1 Hongo, Bunkyo-ku, Tokyo 113-8655, Japan

T. Iwatsubo
Department of Neuropathology, University of Tokyo, 7-3-1 Hongo, Bunkyo-ku, Tokyo 113-8655, Japan

F. Yamashita
Department of Radiology, Iwate Medical University, 2-1-1 Nishitokuta, Yahaba, Iwate 028-3694, Japan

H. Matsuda
Department of Nuclear Medicine, Integrative Brain Imaging Center National Center of Neurology and Psychiatry, 4-1-1, Ogawa-Higashi, Kodaira, Tokyo 187-8551, Japan

and showed no increase with DARTEL normalization for any region of interest (ROI).
Conclusion DARTEL normalization reduces the effect of scanner, which is a major problem in multicenter studies.

Keywords Atlas-based method · Cortex volumetry · Effect of scanner · Magnetic resonance imaging · Statistical Parametric Mapping

Introduction

Cortex volumetry (i.e., atlas-based volumetry [1, 2]) and morphometry (i.e., voxel-based morphometry (VBM) [3]) using three-dimensional T1-weighted magnetic resonance images (3D-T1WIs) with spatial normalization processing have been used to estimate local brain volume in normal subjects [4–7] and in pathological states (e.g., Alzheimer's disease (AD) [8], epilepsy [9], diabetes [10], and panic disorder [11]). However, in these methods, the results of analysis are influenced by image quality. It is reported that image distortion correction [12–15] and image intensity uniformity correction [16–18] can reduce the influence of inferior image quality.

In studies using the cortex segmentation technique, Statistical Parametric Mapping (SPM) [19] is the most commonly used method. The SPM computation algorithms have changed over time (i.e., SPM 99, SPM 2, SPM 5, and SPM 8). Diffeomorphic Anatomical Registration Through Exponentiated Lie Algebra (DARTEL) has recently attracted attention as a groupwise registration algorithm for forming a template for spatial normalization [20].

In dementia with Lewy bodies (DLB), Takahashi et al. [21] reported that analysis with VBM-DARTEL was more accurate and resulted in the detection of more localized morphologic alterations compared with analysis with conventional VBM implemented in SPM 8. They identified a decrease in gray matter volume in the medial temporal lobes in both AD and DLB with VBM-DARTEL; the decrease was greater in patients with AD than in those with DLB. Cuingnet et al. [22] reported that DARTEL significantly improved accuracy for normal controls vs. mild cognitive impairment and normal controls vs. AD compared with SPM 5 unified segmentation.

In healthy subjects, Peelle et al. [23] reported improved registration with DARTEL compared with SPM 5/SPM 8 unified segmentation and found that significant age-related gray matter volume changes were more consistently exhibited in some regions (including bilateral insula) with DARTEL compared with the unified segmentation method.

In a study of very mild AD and healthy controls, Matsuda et al. [24] reported that higher performance for AD diagnosis was achieved with VBM-DARTEL compared with SPM 2. In their report, group comparison between AD and controls showed significant decline of gray matter volume in the left and right parahippocampal gyri with both the SPM 8 and SPM 2 methods. However, cluster size was smaller in SPM 2 compared with DARTEL implemented in SPM 8. In addition, McLaren et al. [25] reported that use of the SPM 5 segmentation algorithm with DARTEL produces more robust and plausible results compared with the FMRIB Automated Segmentation Tool in the FMRIB Software Library (FSL).

DARTEL can now be implemented routinely and simply using the VBM 8 tool (http://dbm.neuro.uni-jena.de/vbm.html) with SPM 8. As mentioned above, it is reported that the DARTEL normalization method reduced the influence of image quality in cortex volumetry analysis. However, previous reports did not show the results of comparison between DARTEL and non-DARTEL normalization regarding the effect of scanner for cortex volumetry with the atlas-based method. Based on the results of previous reports, we predict that the effect of scanner will be reduced with DARTEL. The aim of the present study was to investigate whether the effect of scanner (in the present report, "effect of scanner" means "reproducibility" (i.e., standard deviation of volumes measured with several MRI systems)) is reduced with DARTEL normalization compared with standard normalization, for cortex volumetry using the atlas-based method.

Materials and methods

Subjects and MRI scanning protocol

To investigate the effect of scanner in volume measurement of cortex regions, we acquired 3D-T1WIs of 21 healthy subjects. Subject data are as follows: age (average ± standard deviation), 31.5 ± 7.2 years; 17 males and four females; and no mental disorders, no cognitive impairment, and no episodes of blackouts. 3D-T1WIs of each subject were obtained using each of the following five MRI systems:

1. Siemens system: MRI was performed on a 1.5-T scanner (MAGNETOM Avanto, Siemens Medical Solutions, Erlangen, Germany) with a head matrix coil for reception. MP-RAGE was used to obtain 160 contiguous sagittal 3D-T1WIs with slice thickness of 1.3 mm, repetition time per echo time = 2,400/3.6 ms, inversion time = 1,000 ms, flip angle = 8°, field of view = 24 cm, number of excitations = 1, and pixel matrix 192 × 192.
2. Toshiba system: MRI was performed on a 1.5-T scanner (EXCELART Vantage, Toshiba Medical Systems, Tokyo, Japan) using a quadrature coil for send–receive. MP-RAGE was used to obtain 165 contiguous sagittal 3D-T1WIs with slice thickness of 1.3 mm, repetition time per

echo time = 2,400/4.0 ms, inversion time = 1,000 ms, flip angle = 8°, field of view = 24 cm, number of excitations = 1, and pixel matrix = 192 × 192.

3. GE1.5T system: MRI was performed on a 1.5-T scanner (Signa EXCITE HDx, GE Medical Systems, Waukesha, WI, USA) using a quadrature head coil for send–receive. MP-RAGE was used to obtain 184 contiguous sagittal 3D-T1WIs with slice thickness of 1.3 mm, repetition time per echo time = 3,000/3.9 ms, inversion time = 1,000 ms, flip angle = 8°, field of view = 24 cm, number of excitations = 1, and pixel matrix = 192 × 192.
4. And 5. GE3T PA system and GE3T QD system, respectively. Both systems are 3-T scanners (Signa EXCITE HDx, GE Medical Systems, Waukesha, WI, USA), with the GE3T PA system using a phased-array coil for reception, and the GE3T QD system using a quadrature head coil for send–receive. Otherwise, the conditions were the same for both systems: MP-RAGE was used to obtain 170 contiguous sagittal 3D-T1WIs with slice thickness of 1.3 mm, repetition time per echo time = 2,300 / 2.8 ms, inversion time = 900 ms, flip angle = 8°, field of view = 26 cm, number of excitations = 1, and pixel matrix = 256 × 256.

All 3D-T1WIs were inspected by a board-certified radiologist. None of the following findings was found as a possibility of mis-segmentation on DARTEL normalization and standard normalization, in any subject: brain tumor, infarction, hemorrhage, or brain atrophy. The scanning protocol was approved by the ethical committee of our institution. After the study had been explained to each subject, written informed consent was obtained. Furthermore, to protect subject confidentiality, patient information was stripped from all data.

Image preprocessing for cortex volumetry

3D-T1WIs were processed using the VBM 8 tool implemented in SPM 8. The standard VBM 8 (standard normalization) setting was defined as follows: the affine regularization space template from the International Consortium for Brain Mapping was changed from "European brain" to "East Asian brain" (healthy subjects in the present study are Japanese), the cleanup procedure was changed from "Light Cleanup" to "Through Cleanup"; default settings were used for all other factors. All 3D-T1WIs were segmented into gray matter using two settings: standard normalization and DARTEL normalization. In DARTEL normalization, spatial normalization was set to "High-dimensional: Dartel" from "Low-dimensional: SPM default" on standard normalization setting. For both standard and DARTEL normalization, segmented gray matter images were written as "modulated normalized (affine + nonlinear)".

Cortex volumetry using the regions of interest

Regions of interest (ROIs) were obtained with WFU PickAtlas (Talairach brain atlas theory) [1]. This program automatically generates segmented atlas ROI templates in Montreal Neurological Institute (MNI) space [26]. The ROIs defined in the atlas were originally based on manual delineation of the brain region borders according to the Talairach atlas [1]. Seven bilateral ROI labels provided as default settings by the software were used: "Frontal Lobe," "Hippocampus," "Occipital Lobe," "Orbital Gyrus," "Parietal Lobe," "Putamen," and "Temporal Lobe." ROI volume measurements were obtained using modulated normalized gray matter images.

Statistical analysis for investigation of the effect of scanner

The effect of scanner was evaluated using 110 image sets (i.e., 21 subjects × 5 systems). All image sets were processed with both DARTEL and standard normalization. ROI volumes were then measured on the segmented gray matter images (modulated normalized images) with WFU PickAtlas. We calculated the standard deviations of the seven ROI volume measurements for each subject, for DARTEL, and standard normalization settings for the five scanners. That is, we calculated 294 standard deviations (i.e., 21 subjects × DARTEL and standard normalization settings × 7 ROIs).

Paired Student's t test with the Bonferroni/Dunn method was used to examine the statistical significance of differences in ROI volumes between the standard deviations of DARTEL and standard normalization settings. Statistical significance was set at P value <0.0071.

Additional study for the repeatability of cortex volumetry

It is an important consideration that the present results (i.e., the standard deviations) include the repeatability of cortex volumetry (in the present report, "repeatability" refers to the standard deviation of measured volumes obtained for one MRI system and one subject). Goto et al. [27] reported repeatability of measured brain volume by atlas-based method using T1-weighted image but did not report about DARTEL. Therefore, additional comparison (DARTEL normalization vs. standard normalization) study for the repeatability of cortex volumetry was performed in the present study.

"Subjects and MRI scanning protocol" was the same as "Subjects" and "MRI Scanning Protocol" in the report by Goto et al. [27]. "Image preprocessing for cortex volumetry" and "Cortex volumetry using the regions of interest" were the same as "Image preprocessing for cortex volumetry" and "Cortex volumetry using the regions of interest" in the present report.

"Statistical analysis for investigation of the repeatability" was the same as "Statistical analysis for investigation of the effect of scanner" in the present report. However, calculation

method of standard deviation differed as follows: standard deviation for the five images with five scanners was calculated in the study of the effect of scanner, and standard deviation for the five images with one scanner was calculated in the study of the repeatability.

Results

The standard deviations for each ROI are shown in Fig. 1, while the results of statistical analysis for means of the standard deviations are shown in Table 1. Statistically significant difference was found between standard deviations with DARTEL normalization and those with standard normalization for Frontal Lobe, Occipital Lobe, Orbital Gyrus, Putamen, and Temporal Lobe (paired Student's t test; P value < 0.0071). No significant difference was found in Hippocampus and Parietal Lobe.

For all ROIs, the means of the standard deviations were smaller with DARTEL normalization compared with those with standard normalization. The present results showed that in cortex volumetry using the atlas-based method, the effect of scanner was less with DARTEL normalization compared with standard normalization for Frontal Lobe, Occipital Lobe, Orbital Gyrus, Putamen, and Temporal Lobe; equivalent values were found in Hippocampus and Parietal Lobe; and there was no increase with DARTEL normalization for any ROI in the study.

The results of the mean of the standard deviations for ROI volumes with DARTEL normalization were summarized in Table 2. Each ROI volumes are follows: Frontal Lobe, 563 ml; Hippocampus, 2.09 ml; Occipital Lobe, 171 ml; Orbital Gyrus, 5.69 ml; Parietal Lobe, 215 ml; Putamen, 13.5 ml; and Temporal Lobe, 265 ml.

The results for repeatability of statistical analysis for means of the standard deviations are shown in Table 3. A statistically significant difference was found between standard deviations with DARTEL normalization and those with standard normalization for Hippocampus (paired Student's t test; P value < 0.0071). No significant difference was found in Frontal Lobe, Occipital Lobe, Orbital Gyrus, Parietal Lobe, Putamen, and Temporal Lobe. For Hippocampus, the means of the standard deviations were smaller with standard normalization compared with those with DARTEL normalization. The present results showed that in cortex volumetry using the atlas-based method, high repeatability with standard normalization compared with DARTEL normalization was found in Hippocampus; equivalent repeatability were found in Frontal Lobe, Occipital Lobe, Orbital Gyrus, Parietal Lobe, Putamen, and Temporal Lobe; and low repeatability with standard normalization compared with DARTEL normalization was not found in any ROI in the study.

Discussion

The performance of spatial normalization algorithms is a known limiting factor of semiautomated morphology methods such as atlas- and voxel-based morphometry [3, 28]; a great deal of research effort has recently been applied to modified algorithms that increase reliability [29]. The aim of the present

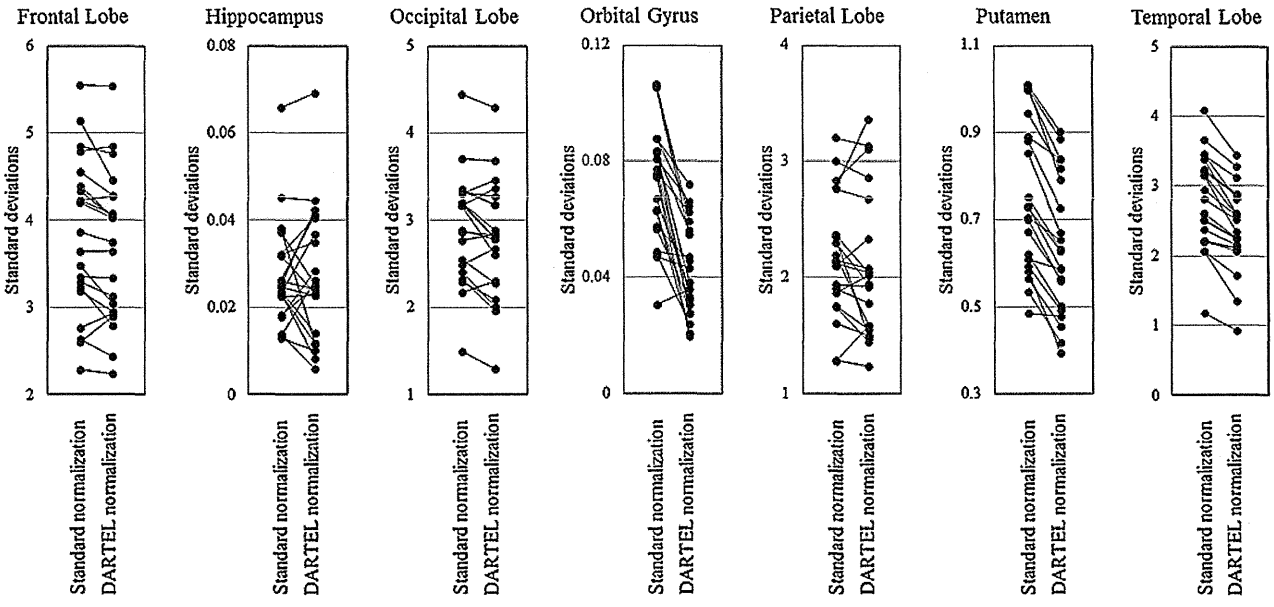

Fig. 1 Effect of scanner for cortex volumetry for standard normalization and DARTEL using the atlas-based method for seven ROIs. *Vertical axis* standard deviation, *horizontal axis* normalization method. The statistical significance of differences between means of the standard deviations for standard normalization and for DARTEL normalization is listed in Table 1

Table 1 Results of statistical analysis of the effect of scanner with standard normalization and with DARTEL for cortex volumetry by the atlas-based method. The mean of effect of scanner (i.e., the standard deviations) with the standard deviations of effect of scanner (i.e., the standard deviations) are shown for each ROI. Statistical significance of differences between standard normalization and DARTEL normalization was analyzed using paired Student's *t* test with the Bonferroni/Dunn method. Statistical significance was set at *P* value <0.0071

ROI name	Standard normalization	DARTEL normalization	*P* value
Frontal lobe	3.84 ± 0.90	3.69 ± 0.86	<0.007
Hippocampus	0.0275 ± 0.0122	0.0271 ± 0.0152	NS
Occipital lobe	2.94 ± 0.63	2.79 ± 0.67	<0.007
Orbital gyrus	0.0717 ± 0.0193	0.0428 ± 0.0161	<0.0001
Parietal lobe	2.17 ± 0.53	2.08 ± 0.61	NS
Putamen	0.756 ± 0.172	0.640 ± 0.158	<0.0001
Temporal lobe	2.79 ± 0.68	2.39 ± 0.61	<0.0001

study was to investigate whether the effect of scanner for cortex volumetry using the atlas-based method was reduced with DARTEL normalization compared with standard normalization as the spatial normalization method.

The present results showed a reduced effect of scanner for cortex volumetry using the atlas-based method for DARTEL normalization compared with standard normalization in Frontal Lobe, Occipital Lobe, Orbital Gyrus, Putamen, and Temporal Lobe; equivalent values in Hippocampus and Parietal Lobe; and showed no increase with DARTEL normalization in any ROI. Reduced effect of scanner produces better cortex volumetry results in multicenter studies because these studies include image data acquired using many different MRI systems. The selected systems differed in terms of static magnetic field strength, reception coil, and manufacturer though we included only five MRI systems in the present study. We found significantly better results for DARTEL normalization than for standard normalization, despite the small number of systems evaluated.

In theory, multicenter studies should have high statistical power because they include a large number of cases. However, several inherent problems of multicenter studies (i.e., signal intensity nonuniformity and distortion of 3D-T1WI) increase variability in measurements, which decreases the statistical power. To minimize variability in measurements, we proposed using correction processing (i.e., nonparametric nonuniform intensity normalization) because nonuniform signal intensity of 3D-T1WI is influenced by coil variation, TR, and uniformity of radio frequency [16, 30, 31]. In addition, to clarify the most suitable methods for correcting for distortion in 3D-T1WI, previous studies investigated whether 3D-T1WI distortion could cause error in brain volume estimation and evaluated the accuracy of various correction methods [12–14].

Table 2 The results of the mean of the standard deviations for ROI volumes with DARTEL normalization

ROI name	Mean of the standard deviations for ROI volumes (%)
Frontal lobe	0.0066
Hippocampus	0.013
Occipital lobe	0.016
Orbital gyrus	0.0075
Parietal lobe	0.0097
Putamen	0.047
Temporal lobe	0.0090

The present results are useful because they indicate that using DARTEL normalization performs better than standard normalization in reducing the problem of effect of scanner for volumetry results in multicenter studies. Moreover, the present result does not contradict those of previous studies that showed improved disease detectability when high-precision DARTEL was used as the spatial normalization method [21–25].

We examined the effect of scanner in DARTEL and non-DARTEL, and showed reduced effect in DARTEL. Image qualities such as image distortion, contrast, and intensity nonuniformity varied among the five systems used in the present study. Previous studies reported a reduction in the influence of inferior image quality when image distortion correction was used [12–15]; greater precision was achieved with the DARTEL spatial registration method developed by Ashburner [20]. Based on these reports, we consider that improved precision of spatial registration reduces the effect of scanner; however, in the present study, the effect of scanner varied according to ROI (i.e., the effect of scanner was reduced in Frontal Lobe, Occipital Lobe, Orbital Gyrus, Putamen, and Temporal Lobe for DARTEL compared with non-DARTEL but was equivalent between Hippocampus and Parietal Lobe).

Pereira et al. reported that registration accuracy is not uniform across the brain [32]. These findings are consistent with the present results (i.e., ROI dependence). Pereira et al. also reported that deep structures are more challenging to

Table 3 The results of statistical analysis of the repeatability with standard normalization and with DARTEL for cortex volumetry by the atlas-based method. The mean of the repeatability (i.e., the standard deviations) with the standard deviations of the repeatability (i.e., the standard deviations) are shown for each ROI. Statistical significance of differences between standard normalization and DARTEL normalization was analyzed using paired Student's *t* test with the Bonferroni/Dunn method. Statistical significance was set at *P* value <0.0071

ROI name	DARTEL normalization	Standard normalization	*P* value
Frontal lobe	1.03 ± 0.80	1.10 ± 0.86	NS
Hippocampus	0.0171 ± 0.0132	0.0103 ± 0.0059	<0.007
Occipital lobe	0.541 ± 0.360	0.593 ± 0.383	NS
Orbital gyrus	0.0177 ± 0.0140	0.0322 ± 0.0292	NS
Parietal lobe	0.743 ± 0.616	0.656 ± 0.590	NS
Putamen	0.160 ± 0.095	0.167 ± 0.105	NS
Temporal lobe	0.549 ± 0.505	0.641 ± 0.439	NS

register because of the lack of clearly defined boundaries when compared with the external brain surface [32]. These findings are inconsistent with our results because we found no significant reduced effect of scanner in Parietal Lobe as a surface region. It is difficult to clarify the cause of this inconsistency, but we think that low repeatability may hide the findings for significant reduced effect of scanner in the present study. In fact, low repeatability was found for Hippocampus and Parietal Lobe, and was not found for other ROIs.

It is an important consideration that the present results for effect of scanner (i.e., the standard deviations) include the repeatability of cortex volumetry. Low repeatability increases the standard deviation of the measured values and could have increased the standard deviation in the present results. However, in the results for repeatability (see Table 3), equivalent repeatability with DARTEL normalization compared with standard normalization was found for all ROIs, except for Hippocampus. Therefore, we conclude that the main reason for reduced effect of scanner found in the present study is "reduced effect of scanner" and not "improved repeatability."

It is important to know the standard deviations of measured values for ROI volume. For example, if the standard deviation is 0.1 ml, we consider that measurement error by standard deviation poses no problem for the detection sensitivity of cortex volume changes with a ROI of 1,000 ml. However, if the standard deviation is 0.1 ml, measurement error by standard deviation is a problem for the detection sensitivity of cortex volume changes with a ROI of 0.3 ml. For this reason, additional results are presented in Table 2, in which Putamen shows the highest value among means of the standard deviations for ROI volume.

The high iron deposition in the putamen compared with other regions is probably responsible for this finding [33]. In addition, iron deposition levels differ between the anterior and posterior regions of the putamen. Ferritin and hemosiderin molecules in tissue both increase R2 and R2* (transverse relaxation), and signal intensity in 3D-T1WI is influenced by changes in transverse relaxation time [34]. Also, segmentation with SPM is based mainly on the frequency distribution of the signal intensity of 3D-T1WI and nonlinear registration with tissue probability maps [19]. Typically, the probability that a voxel contains gray matter is determined by the voxel intensity and location of the voxel in the brain, with reference to prior probability maps. It is known that variation in signal intensity causes segmentation errors. This variation was confirmed in the present study as speckled signal distribution in the putamen region of segmented gray matter images. That is, even if SPM with DARTEL is used for cortex segmentation, segmentation of the putamen may be too imprecise to detect relatively small volume change in longitudinal volumetric studies.

The main limitation of the present study is the lack of a gold standard with which the segmentation methods can be compared. In addition, conclusions regarding the relative superiority of any approach are tentative and may be affected greatly by modifying the parameters of each approach. However, the present results indicate that more reliable analytic results can be obtained in multicenter studies when DARTEL is used as the spatial normalization method compared with standard normalization.

Conclusions

To our knowledge, this is the first study to compare DARTEL and standard normalization in terms of the effect of scanner for cortex volumetry with the atlas-based method. The results show reduced effect of scanner for DARTEL normalization compared with standard normalization. This result is useful because it indicates that the use of DARTEL rather than standard normalization reduces one of the problems (i.e., effect of scanner in analytical results) encountered in multicenter studies.

Acknowledgments This study was supported by a Grant-in-Aid for Scientific Research on Innovative Areas (Comprehensive Brain

Science Network) from the Ministry of Education, Science, Sports and Culture of Japan.

Conflict of interest We declare that we have no conflict of interest.

References

1. Maldjian JA, Laurienti PJ, Kraft RA et al (2003) An automated method for neuroanatomic and cytoarchitectonic atlas-based interrogation of fMRI data sets. Neuroimage 19:1233–1239
2. Gonoi W, Abe O, Yamasue H, et al. (2009) Age-related changes in regional brain volume evaluated by atlas-based method. Neuroradiology
3. Ashburner J, Friston KJ (2000) Voxel-based morphometry—the methods. Neuroimage 11:805–821
4. Good CD, Johnsrude I, Ashburner J et al (2001) Cerebral asymmetry and the effects of sex and handedness on brain structure: a voxel-based morphometric analysis of 465 normal adult human brains. Neuroimage 14:685–700
5. Nunnemann S, Wohlschlager AM, Ilg R et al (2009) Accelerated aging of the putamen in men but not in women. Neurobiol Aging 30:147–151
6. Sato K, Taki Y, Fukuda H et al (2003) Neuroanatomical database of normal Japanese brains. Neural Netw 16:1301–1310
7. Draganski B, Gaser C, Busch V et al (2004) Neuroplasticity: changes in grey matter induced by training. Nature 427:311–312
8. Baron JC, Chetelat G, Desgranges B et al (2001) In vivo mapping of gray matter loss with voxel-based morphometry in mild Alzheimer's disease. Neuroimage 14:298–309
9. Keller SS, Roberts N (2008) Voxel-based morphometry of temporal lobe epilepsy: an introduction and review of the literature. Epilepsia 49:741–757
10. Musen G, Lyoo IK, Sparks CR et al (2006) Effects of type 1 diabetes on gray matter density as measured by voxel-based morphometry. Diabetes 55:326–333
11. Hayano F, Nakamura M, Asami T et al (2009) Smaller amygdala is associated with anxiety in patients with panic disorder. Psychiatry Clin Neurosci 63:266–276
12. Doran SJ, Charles-Edwards L, Reinsberg SA et al (2005) A complete distortion correction for MR images: I. Gradient warp correction. Phys Med Biol 50:1343–1361
13. Janke A, Zhao H, Cowin GJ et al (2004) Use of spherical harmonic deconvolution methods to compensate for nonlinear gradient effects on MRI images. Magn Reson Med 52:115–122
14. Jovicich J, Czanner S, Greve D et al (2006) Reliability in multi-site structural MRI studies: effects of gradient non-linearity correction on phantom and human data. Neuroimage 30:436–443
15. Goto M, Abe O, Kabasawa H et al (2012) Effects of image distortion correction on voxel-based morphometry. Magn Reson Med Sci 11:27–34
16. Sled JG, Zijdenbos AP, Evans AC (1998) A nonparametric method for automatic correction of intensity nonuniformity in MRI data. IEEE Trans Med Imaging 17:87–97
17. Arnold JB, Liow JS, Schaper KA et al (2001) Qualitative and quantitative evaluation of six algorithms for correcting intensity nonuniformity effects. Neuroimage 13:931–943
18. Vovk U, Pernus F, Likar B (2007) A review of methods for correction of intensity inhomogeneity in MRI. IEEE Trans Med Imaging 26:405–421
19. Ashburner J, Friston KJ (2005) Unified segmentation. Neuroimage 26:839–851
20. Ashburner J (2007) A fast diffeomorphic image registration algorithm. Neuroimage 38:95–113
21. Takahashi R, Ishii K, Miyamoto N et al (2010) Measurement of gray and white matter atrophy in dementia with Lewy bodies using diffeomorphic anatomic registration through exponentiated lie algebra: a comparison with conventional voxel-based morphometry. AJNR Am J Neuroradiol 31:1873–1878
22. Cuingnet R, Gerardin E, Tessieras J et al (2011) Automatic classification of patients with Alzheimer's disease from structural MRI: a comparison of ten methods using the ADNI database. Neuroimage 56:766–781
23. Peelle JE, Cusack R, Henson RN (2012) Adjusting for global effects in voxel-based morphometry: gray matter decline in normal aging. Neuroimage 60:1503–1516
24. Matsuda H, Mizumura S, Nemoto K et al (2012) Automatic voxel-based morphometry of structural MRI by SPM8 plus diffeomorphic anatomic registration through exponentiated lie algebra improves the diagnosis of probable Alzheimer Disease. AJNR Am J Neuroradiol 33:1109–1114
25. McLaren DG, Kosmatka KJ, Kastman EK et al (2010) Rhesus macaque brain morphometry: a methodological comparison of voxel-wise approaches. Methods 50:157–165
26. Tzourio-Mazoyer N, Landeau B, Papathanassiou D et al (2002) Automated anatomical labeling of activations in SPM using a macroscopic anatomical parcellation of the MNI MRI single-subject brain. Neuroimage 15:273–289
27. Goto M, Miyati T, Abe O et al (2012) Repeatability of measured brain volume by atlas-based method using T1-weighted image. J Digit Imaging 25:173–178
28. Bookstein FL (2001) "Voxel-based morphometry" should not be used with imperfectly registered images. Neuroimage 14:1454–1462
29. Acosta-Cabronero J, Williams GB, Pereira JM et al (2008) The impact of skull-stripping and radio-frequency bias correction on grey-matter segmentation for voxel-based morphometry. Neuroimage 39:1654–1665
30. Rojas R, Rodriguez AO (2007) Numerical study of the SNR and SAR of MRI coil arrays. Conf Proc IEEE Eng Med Biol Soc 2007:1196–1199
31. Simmons A, Tofts PS, Barker GJ et al (1994) Sources of intensity nonuniformity in spin echo images at 1.5 T. Magn Reson Med 32:121–128
32. Pereira JM, Xiong L, Acosta-Cabronero J et al (2010) Registration accuracy for VBM studies varies according to region and degenerative disease grouping. Neuroimage 49:2205–2215
33. Hallgren B, Sourander P (1958) The effect of age on the non-haemin iron in the human brain. J Neurochem 3:41–51
34. Schenck JF (2003) Magnetic resonance imaging of brain iron. J Neurol Sci 207:99–102

INTERNAL MEDICINE

□ CASE REPORT □

Postanoxic Akinesia with Bilateral Pallidal Lesions: A PET Study

Shunsuke Kobayashi[1,4], Toshimitsu Momose[2], Masaki Sakurai[3,4] and Ichiro Kanazawa[4]

Abstract

A 70-year-old woman developed marked akinesia after an anoxic event related to bronchiectasia. Magnetic resonance imaging studies revealed lesions in the bilateral globus pallidus and, to a lesser extent, in the putamen. Positron emission tomography studies with ^{18}F-6-fluoro-*L*-dopa and ^{11}C-*N*-methylspiperone showed a decreased pre- and post-synaptic uptake in the striatum. Consistent with previous reports, the present case demonstrated the basal ganglia, particularly the globus pallidus, to be selectively susceptible to anoxic insults. Furthermore, a PET study indicated a disrupted presynaptic integrity of the dopaminergic terminals and decreased dopamine D_2 receptor binding, which together appear to underlie the pathophysiology of post-anoxic akinesia, at least in the present case.

Key words: Parkinsonism, akinesia, anoxia, globus pallidus, dopamine, positron emission tomography

(Intern Med 51: 2449-2451, 2012)
(DOI: 10.2169/internalmedicine.51.8008)

Introduction

Anoxia is a cause of brain damage distinct from ischemia and other neurotoxic insults, such as carbon monoxide poisoning. The clinical details of anoxic brain injury remain unclear, because anoxia often accompanies ischemia and only on rare occasions causes purely anoxic brain injury, including accidents during anesthesia, drowning, altitude disease, and respiratory failure. We herein report a patient who suffered from severe anoxia and developed akinesia. We studied her anatomic lesions by magnetic resonance imaging (MRI) and dopamine transmission with positron emission tomography (PET) using ^{18}F-6-fluoro-*L*-dopa (^{18}F-DOPA) and ^{11}C-*N*-methylspiperone (^{11}C-NMSP) as tracers.

Case Report

A 70-year-old woman developed massive hemoptysis. Prior to this event, she was ambulatory with a normal intellect. She had no remarkable past medical history except for having suffered from bronchiectasia for 30 years. On arrival, she was cyanotic and comatose with feeble respiration. The results of the initial arterial blood gas examination showed a pH of 6.74, $PaCO_2$ of 114 mmHg and PaO_2 of 34.6 mmHg. Her blood pressure was maintained at a normal level. She gradually regained consciousness within two days. A CT study four days after the onset exhibited a low density area in the bilateral lentiform nuclei. Two years after the event, she was referred to our department with a chief complaint of gait disturbance. A general examination revealed fine crackles in the lower lung fields. A full blood count indicated microcytic hypochromic anemia, but the results of other routine blood tests were unremarkable, including the plasma copper and ceruloplasmin level. Neurologically, she was conscious and well oriented. Her intelligence score on the Wechsler Adult Intelligence Scale Revised (WAIS-R) scale was 79 (verbal IQ 79, performance IQ 78) and she had 23/26 correct responses in Raven's Colored Progressive Matrices test (RCPM). She showed severe akinesia and an impaired postural reflex. Her muscle rigidity was minimal. She showed frequent gait freezing, particularly on initiation and turning. Her gait freezing markedly improved when she walked on stripes drawn on the floor. Her voice was se-

[1]Department of Neurology, School of Medicine, Fukushima Medical University, Japan, [2]Department of Radiology, Graduate School of Medicine, University of Tokyo, Japan, [3]Department of Physiology, Teikyo University School of Medicine, Japan and [4]Department of Neurology, Division of Neuroscience, Graduate School of Medicine, University of Tokyo, Japan
Received for publication April 19, 2012; Accepted for publication June 17, 2012
Correspondence to Dr. Shunsuke Kobayashi, skoba-tky@umin.net

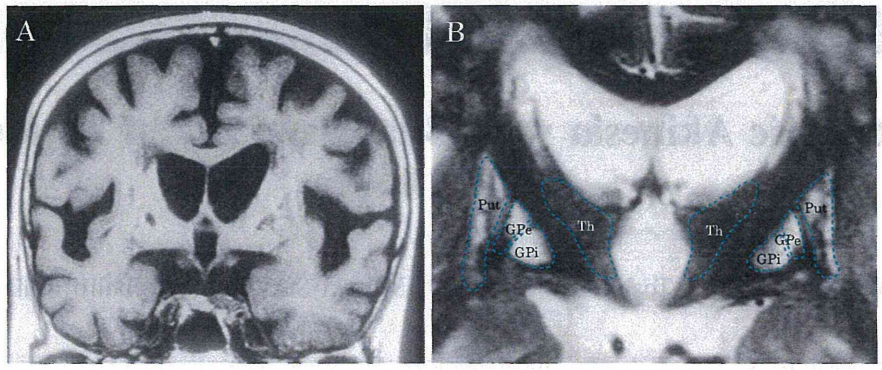

Figure 1. Brain MRI two years after the hypoxic event. Coronal sections of T1-weighted (A) and T2-weighted (B) images showed bilateral lesions in the putamen (Put), internal globus pallidus (GPi) and external globus pallidus (GPe), and periventricular white matter. Th: thalamus

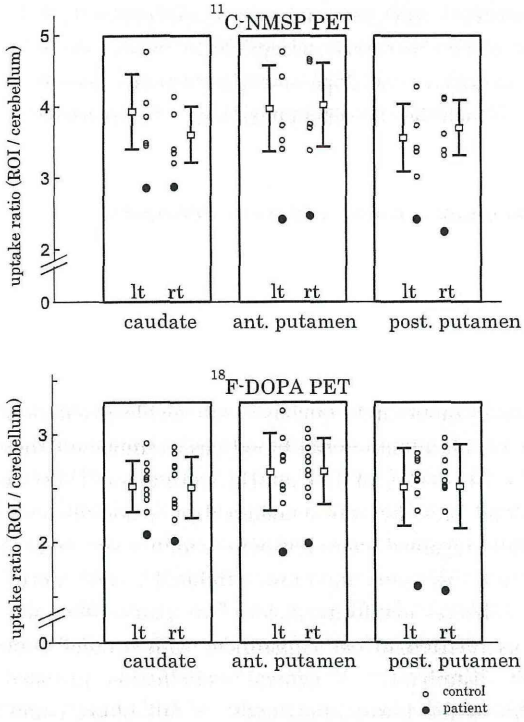

Figure 2. The results of ^{11}C-NMSP and ^{18}F-DOPA PET studies. The tracer uptakes in three ROIs (caudate nucleus, anterior putamen and posterior putamen) were normalized to the uptake value in the cerebellum and expressed as the uptake ratio. Closed and open circles indicate the uptake ratios of the present patient and normal control subjects, respectively. Error bars: standard deviation (SD) of normal control data.

verely hypophonic, no more than whispering. She also had a mask-like face. Her glabellar tap reflex was markedly enhanced and a snout reflex was present. Micrographia was also evident. She showed no weakness and her sensation, coordination, and deep tendon reflexes were normal. Her symptoms poorly responded to levodopa and other dopamine agonists, but her gait freezing mildly improved after the administration of L-threo-3,4-dihydroxyphenylserine.

An MRI study showed T2 high and T1 low signal lesions in the bilateral globus pallidus, and to a lesser extent in the putamen (Fig. 1). A magnetic resonance angiography study revealed no significant stenosis in the major vessels. PET studies with ^{11}C-NMSP and ^{18}F-DOPA were conducted on separate days in the absence of dopaminergic treatment (HEADTOME-IV, Shimazu, Kyoto, Japan). The radioactivity in six regions of interest (ROIs; bilateral caudate nucleus, anterior and posterior parts of the putamen) was sampled (1). The uptake in each ROI was compared to the non-specific retention in the cerebellum at 90 minutes for ^{11}C-NMSP and at 120 minutes for ^{18}F-DOPA. When compared with healthy control subjects (n=5; age 68.8±8.3 [mean ± SD]), the ^{11}C-NMSP uptake ratios of our patient were markedly decreased bilaterally in all ROIs ($p<0.01$, t-test; Fig. 2, top). For the ^{18}F-DOPA PET study, the control group included subjects with a wide range of ages (n=9; age 20 to 81; 38.7±26.8 [mean ± SD]), because age does not influence the ^{18}F-DOPA PET data in any of the ROIs used in this study ($p>0.17$, Pearson's test). The ^{18}F-DOPA uptake ratios of our patient were significantly lower than those of the control group in all ROIs (Fig. 2, bottom).

Discussion

Our patient developed marked akinesia and postural disturbance after severe hypoxia. The results of the WAIS-R and RCPM indicated that her cognitive functions were relatively preserved. Therefore, her akinesia cannot be explained by cognitive impairment or decreased motivation, but likely were attributable to parkinsonism due to basal ganglia lesions. Similar cases have been reported with isolated lesions in the bilateral globus pallidus (GP), particularly in the external globus pallidus (GPe) (2-4). The clinical course and the results of neuroimaging studies suggest that other causes of akinesia are unlikely, including normal pressure hydrocephalus, idiopathic and drug-induced parkinsonism, progressive supranuclear palsy, corticobasal degeneration, and Wilson's disease.

According to the standard physiological model of the basal ganglia, the GPe is a key station of the indirect pathway,

and its damage would lead to a net reduction in the basal ganglia output to the thalamus through disinhibition of the subthalamic nucleus and increased excitation of the internal segment of GP (GPi) (5, 6). Therefore, akinesia due to GPe lesions can thus be explained by this model. On the other hand, GPi lesions apparently ameliorate parkinsonism, as proven by therapeutic pallidotomy in Parkinson disease patients. In our patient, it was difficult to specify the lesions responsible for the akinesia because of the presence of other lesions in the basal ganglia (Fig. 1B). Based on the pathophysiological theory of parkinsonism, we speculated that the adverse effect of GPe lesions may have overwhelmed the anti-parkinsonian effect of the GPi lesions in this patient. Previous studies of anoxic brain damage have also showed that akinesia is associated with GP lesions, while dystonia patients tend to have lesions in the putamen (7, 8).

Besides the anatomical lesions in the basal ganglia, the PET study performed on our patient revealed the functional blockade of dopamine transmission. Striatal D_2 receptor binding was decreased in our patient, which is in contrast to the findings observed in Parkinson's disease patients who show increased striatal D2 receptor binding in the absence of dopaminergic treatment (9, 10).

The striatum and globus pallidus are also susceptible to neurotoxic insults by carbon monoxide, cyanide, and manganese (8, 11, 12). However, little is known about dopamine transmission in these clinical settings. Yoshii and colleagues conducted a ^{11}C-NMSP PET study with a victim of carbon oxide (CO) poisoning with bilateral pallidal lesions (13). Unlike our case, the parkinsonism of their patient responded well to bromocriptine treatment, and a PET study revealed an increased D_2 receptor binding potential in the striatum. The responsiveness to dopaminergic treatment may therefore be variable in postanoxic and neurotoxic akinesia, perhaps depending on the severity, lesioned structures, and etiologies. Dopamine PET may therefore predict the responsiveness to dopaminergic treatment for akinesia.

Hypoxia is also known to cause parkinsonism in association with nigral damage. Diffusion-weighted MRI in postanoxic patients showed decreased regional Apparent Diffusion Coefficient in the substantia nigra, thus indicating cytotoxic edema (14, 15). The substantia nigra (SNc) may be vulnerable to hypoxia because of its high iron content and direct binding of carbon monoxide to heme iron. It is also possible that the decreased ^{18}F-DOPA uptake reflects some degree of anoxic damage in the SNc.

In summary, postanoxic parkinsonism may result from damage to multiple brain structures, including the GP, putamen, and SNc. Dopamine PET may be useful in future studies to clarify how the various forms of postanoxic parkinsonism correlate with the clinical manifestations and drug responsiveness.

The authors state that they have no Conflict of Interest (COI).

References

1. Yoshimura M, Yamamoto T, Iso-o N, et al. Hemiparkinsonism associated with a mesencephalic tumor. J Neurol Sci **197**: 89-92, 2002.
2. Féve AP, Fénelon G, Wallays C, Rémy P, Guillard A. Axial motor disturbances after hypoxic lesions of the globus pallidus. Mov Disord **8**: 321-326, 1993.
3. Kuoppamäki M, Rothwell JC, Brown RG, Quinn N, Bhatia KP, Jahanshahi M. Parkinsonism following bilateral lesions of the globus pallidus: performance on a variety of motor tasks shows similarities with Parkinson's disease. J Neurol Neurosurg Psychiatry **76**: 482-490, 2005.
4. Hawker K, Lang AE. Hypoxic-ischemic damage of the basal ganglia. Case reports and a review of the literature. Mov Disord **5**: 219-224, 1990.
5. Obeso JA, Rodriguez-Oroz MC, Rodriguez M, et al. Pathophysiology of the basal ganglia in Parkinson's disease. Trends Neurosci **23**: S8-S19, 2000.
6. Alexander GE, Crutcher MD. Functional architecture of basal ganglia circuits: neural substrates of parallel processing. Trends Neurosci **13**: 266-271, 1990.
7. Bhatt MH, Obeso JA, Marsden CD. Time course of postanoxic akinetic-rigid and dystonic syndromes. Neurology **43**: 314-317, 1993.
8. Bhatia KP, Marsden CD. The behavioural and motor consequences of focal lesions of the basal ganglia in man. Brain **117**: 859-876, 1994.
9. Rinne UK, Lonnberg P, Koskinen V. Dopamine receptors in the Parkinsonian brain. J Neural Transm **51**: 97-106, 1981.
10. Guttman M, Seeman P. L-dopa reverses the elevated density of D2 dopamine receptors in Parkinson's diseased striatum. J Neural Transm **64**: 93-103, 1985.
11. Cersosimo Cersosimo MG, Koller WC. The diagnosis of manganese-induced parkinsonism. Neurotoxicology **27**: 340-346, 2006.
12. Carella F, Grassi MP, Savoiardo M, Contri P, Rapuzzi B, Mangoni A. Dystonic-Parkinsonian syndrome after cyanide poisoning: clinical and MRI findings. J Neurol Neurosurg Psychiatry **51**: 1345-1348, 1988.
13. Yoshii F, Kozuma R, Takahashi W, Haida M, Takagi S, Shinohara Y. Magnetic resonance imaging and ^{11}C-N-methylspiperone/positron emission tomography studies in a patient with the interval form of carbon monoxide poisoning. J Neurol Sci **160**: 87-91, 1998.
14. Kinoshita T, Sugihara S, Matsusue E, Fujii S, Ametani M, Ogawa T. Pallidoreticular damage in acute carbon monoxide poisoning: diffusion-weighted MR imaging findings. Am J Neuroradiol **26**: 1845-1848, 2005.
15. Lou M, Jing CH, Selim MH, Caplan LR, Ding MP. Delayed substantia nigra damage and leukoencephalopathy after hypoxic-ischemic injury. J Neurol Sci **277**: 147-149, 2009.

Journal of Psychiatric Research 46 (2012) 1590–1594

Contents lists available at SciVerse ScienceDirect

Journal of Psychiatric Research

journal homepage: www.elsevier.com/locate/psychires

The high frequency of periodic limb movements in patients with Lewy body dementia

Shinichiro Hibi [a], Yasuhiro Yamaguchi [a,*], Yumi Umeda-Kameyama [a], Hiroshi Yamamoto [a], Katsuya Iijima [a], Toshimitsu Momose [b], Masahiro Akishita [a], Yasuyoshi Ouchi [a]

[a] Department of Geriatric Medicine, Graduate School of Medicine, The University of Tokyo, 7-3-1 Hongo, Bunkyo-ku, Tokyo 113-0033, Japan
[b] Department of Radiology, Graduate School of Medicine, The University of Tokyo, Bunkyo-ku, Tokyo, Japan

ARTICLE INFO

Article history:
Received 12 January 2012
Received in revised form
5 July 2012
Accepted 9 July 2012

Keywords:
Periodic limb movements
Dementia with Lewy bodies
Alzheimer's disease
REM sleep behavior disorder
Polysomnographic recordings

ABSTRACT

Background: Although dementia with Lewy bodies (DLB) is the second most common form of neurodegenerative dementia after Alzheimer's disease (AD), the clinical diagnosis is frequently difficult. Because both REM sleep behavior disorders and Parkinson's disease also have alpha-synucleinopathy similar to DLB, and show an increase in periodic limb movements (PLM), we evaluated the association between DLB and PLM, which may serve as an additional information to differentiate AD and DLB.
Methods: Overnight polysomnographic recordings were performed for the inpatients in our hospital who were suspected to have dementia. The quality of sleep, oxygen-desaturation index and periodic limb movements were compared among the patients clinically diagnosed with DLB, AD or as having no dementia.
Results: Nine DLB patients, twelve AD patients and ten non-demented patients were enrolled in the study. The number of PLM during sleep per hour of total sleep time (PLMS index) was significantly higher in the DLB patients than the AD patients or the non-demented patients. No significant differences were found between the AD patients and the non-demented patients. To differentiate DLB from AD, a PLMS index of more than 15.0 had a sensitivity of 88.9% and a specificity of 83.3%.
Conclusions: The DLB patients exhibited a higher PLMS index than the AD patients, and this index could be clinically useful for the diagnostic differentiation of DLB from AD.

1. Introduction

Dementia with Lewy bodies (DLB) is the second most common form of neurodegenerative dementia after Alzheimer's disease (AD), affecting 15–25% of elderly demented patients (McKeith et al., 1996). DLB is characterized by intracytoplasmic inclusions called Lewy bodies, which consist of filamentous protein granules composed of alpha-synuclein and ubiquitin. Although the pathological diagnosis of DLB can be made based on the observation of Lewy body deposit throughout the cortex and subcortical regions, this is not generally possible except during autopsy.

The clinical diagnostic criteria for DLB were first published in 1996 (McKeith et al., 1996), and were modified in 2005 (McKeith et al., 2005). The central or core symptoms in DLB are progressive cognitive decline, recurrent visual hallucinations, spontaneous features of parkinsonism, and fluctuating cognition. These diagnostic criteria require a clinical evaluation by a trained neurologist and include few objective markers. Although Single Photon Emission Computed Tomography (SPECT) and ^{123}I-metaiodobenzylguanidine (MIBG) myocardial scintigraphy are useful in the differential diagnosis of DLB (Lobotesis et al., 2001; Colloby et al., 2002; Yoshita et al., 2001; Hanyu et al., 2006), these examinations are too expensive to be generally utilized.

DLB is frequently complicated with REM sleep behavior disorder (RBD) (McKeith et al., 2005; Boeve et al., 2001, 2003, 2007; Gagnon et al., 2006), which is characterized by an increase in periodic limb movements (PLM) (Fantini et al., 2002). Some reports have also indicated that there is an increase of PLM in patients with Parkinson's disease (PD) (Wetter et al., 2000; Lavault et al., 2009). In addition, both RBD and PD are alpha-synucleinopathies, similar to DLB.

The pathophysiology of PLM is not well understood. In addition to RBD and PD, some studies have also shown that advancing age is associated with PLM (Coleman et al., 1981; Ancoli-Israel et al., 1991). Furthermore, Rose et al. have suggested that there is an increase of PLM in severely demented patients (Rose et al., 2011).

* Corresponding author. Tel.: +81 3 5800 8652; fax: +81 3 5800 6530.
E-mail address: yamayasu-tky@umin.ac.jp (Y. Yamaguchi).

0022-3956/$ – see front matter © 2012 Elsevier Ltd. All rights reserved.
http://dx.doi.org/10.1016/j.jpsychires.2012.07.007

However, these hypotheses have not yet been systematically studied, and no controlled data have been published to date.

We hypothesized that the patients with DLB would exhibit a higher frequency of PLM compared to the demented patients with AD, and evaluated the usefulness of PLM measurement as a novel tool for the differential diagnosis of dementia. As a result, we observed that patients with DLB exhibited a significantly higher PLMS index compared to patients with AD.

2. Methods

2.1. Subjects

The study population was comprised of the consecutive inpatients of the Department of Geriatric Medicine at the University of Tokyo Hospital, who were admitted for the evaluation of progressive cognitive impairment. The patients underwent neuropsychological assessments, including the Mini-Mental State Examination (MMSE), Frontal Assessment Battery and Clock Draw Test. They also underwent blood tests and neuroimaging tests, such as Magnetic Resonance Imaging (MRI) and SPECT. The diagnosis was made at a consensus conference of physicians and neurologists, based on the clinical diagnostic criteria for DLB proposed by McKeith et al. in 2005 (McKeith et al., 2005), and the National Institute of Neurological and Communicative Disorders and Stroke and the Alzheimer's disease and Related Disorders Association (NINCDS-ADRDA) (McKhann et al., 1984). The patients with probable DLB and possible DLB were included in the DLB group. The non-demented group comprised the patients who did not fit the criteria for dementia in the medical and neurological examinations. Patients with cognitive impairments other than AD or DLB (e.g., normal pressure hydrocephalus, vascular dementia) were excluded from the study.

From November 2010 to September 2011, 43 patients were enrolled in this study. We excluded the 4 patients whose recorded total sleep time was less than two hours. In addition, we excluded five patients who were taking antipsychotics, antidepressants, levodopa, dopamine-agonists and clonazepam, for those drugs could have some effect on the PLM.

The study was approved by the institutional review board of the Graduate School of Medicine, University of Tokyo, and written informed consent was obtained from all participants before the study.

2.2. Polysomnography

The patients underwent overnight polysomnographic recordings in the inpatient ward. Thirty of the 31 patients underwent polysomnography at least three days after admission. The remaining patient, who was in the non-demented group, underwent polysomnography on an adaptation night. The recordings included two electroencephalogram (EEG) leads (C3–A2 and O2–A1), an electrooculogram (EOG) and submental electromyogram (EMG). Nasal and oral thermistor channels, arterial oxygen saturation (finger oximetry) and an EMG of both anterior tibialis muscles were also monitored (Somnotrac Pro, CareFusion, USA). All sleep recordings were scored visually by an experienced rater according to the standard criteria (Iber et al., 2007).

PLM were scored during sleep in accordance with international scoring rules (Zucconi et al., 2006). PLM were defined as four or more consecutive leg movements, which lasted 0.5–10 s, the interval of which was 5–90 s. Leg movements following apneas or hypopneas were excluded. Respiratory events were scored according to AASM guidelines (Iber et al., 2007). Sleep apneas were defined as complete cessation of airflow >10 s. Hypopneas were defined as a reduction ≥50% in airflow plus ≥3% drop in SpO_2 and/or a micro arousal. The apneas-hypopneas index (AHI) was calculated as the number of apneas and hypopneas per sleep hour. In some patients who removed the airflow sensor, oxygen desaturation of 3% or more was substituted to exclude the leg movements associated with breathing disorders and to calculate the AHI. Sleep efficiency, which was defined as the ratio of total sleep time to time in bed, was also calculated.

The number of PLM during sleep per hour of total sleep time (the PLMS index), the apneas-hypopneas index and the number of occasions of oxygen desaturation of 3% or more per hour of total sleep time (3%ODI) were calculated.

The patients who had REM sleep without atonia on polysomnography and had a history of harmful behaviors in sleep were diagnosed with RBD according to the diagnostic criteria (Iber et al., 2007).

2.3. Statistical analysis

The distribution of data was examined using the Shapiro–Wilk test. If data were normally distributed, a one way analysis of variance with Games-Howell post-hoc tests were applied for group comparisons. If the data deviated significantly from normality, the Kruskal–Wallis test was used, followed by evaluation with the Mann–Whitney U test for multiple comparisons, with the p values being corrected according to the Bonferroni method. The χ^2 test was used to compare categorical variables, such as gender and the number of RBD patients.

The diagnostic cutoff points for the PLMS index to discriminate between DLB and AD were estimated for each outcome by maximizing the Youden index. The discrimination ability was assessed by the area under the curve (AUC). Using this threshold, the sensitivity and specificity were calculated.

All of the statistical analyses were performed using the SPSS software program (version 19.0, SPSS inc., Chicago). Statistical significance was defined as p values < 0.05.

3. Results

3.1. Patients

Nine patients with DLB, twelve patients with AD and ten non-demented patients were enrolled in the study. Among the nine patients in the DLB group, five patients had probable DLB and four patients had possible DLB. The diagnoses in the four possible DLB patients were all supported by the typical findings in SPECT; generalized low uptake, reduced occipital activity, and relatively preserved hippocampal blood flow. In addition, three of the four possible DLB patients underwent MIBG myocardial scintigraphy and all showed low uptake. Table 1 shows the characteristics of the subjects. The age, sex distributions, and renal function were not significantly different among the three groups. No significant difference was found between the DLB group and the AD group ($p = 0.337$) in the MMSE. The use of medications for hypertension, hyperlipidemia and diabetes mellitus were similar between the groups. Two patients in the DLB group, two patients in the AD group and no patients in the non-demented group had taken donepezil. None of the patients fit the diagnostic criteria for restless legs syndrome (Allen et al., 2003).

3.2. Findings of polysomnography

The sleep and respiratory measurements are shown in Table 2. There were no significant differences in the percentage of Stage N3 or the percentage of REM sleep among the three groups. As

Table 1
Characteristics of DLB patients, AD patients and non-demented patients.

Characteristics	DLB patients	AD patients	Non-demented	*p* value
Number of subjects	$n = 9$	$n = 12$	$n = 10$	
Age (years)	82.9 ± 5.9	80.9 ± 6.2	79.1 ± 4.5	n.s.
Sex (men/women)	4/5	3/9	3/7	n.s.
MMSE	22.4 ± 3.5	20.3 ± 3.3	27.8 ± 2.1	<0.001*
Serum creatinine (mg/dl)	0.74 ± 0.27	0.74 ± 0.22	0.67 ± 0.15	n.s.
Hypertension	3 (33.3)	4 (25.0)	5 (50.0)	n.s.
Hyperlipidemia	1 (11.1)	1 (8.3)	1 (10.0)	n.s.
Diabetes mellitus	1 (11.1)	1 (8.3)	3 (30.0)	n.s.

Values expressed as mean ± standard deviation or number (%). * = one way analysis of variance with Games-Howell post-hoc tests: DLB vs AD $p = 0.337$, DLB vs non-demented $p = 0.005$, AD vs non-demented $p < 0.001$. AD = Alzheimer's disease; DLB = Dementia with Lewy bodies; MMSE = Mini-mental State Examination; n.s. = not significant.

expected, the prevalence of RBD was significantly higher in the DLB group compared to the AD group or the non-demented group ($p = 0.004$). The AHI and 3%ODI was slightly higher in the AD group compared to the DLB group and the non-demented group, but the difference was not statistically significant.

The observed PLMS indices are shown in Fig. 1. The patients in the DLB group had a significantly higher PLMS index compared to the patients in the AD group and those in the non-demented group. No significant differences in the PLMS index were found between the AD group and the non-demented group. The PLMS indices of the four DLB patients with RBD were 27.8, 147.8, 43.7 and 149.3, respectively. After the exclusion of these four DLB patients with RBD, there was also a statistically significant difference in the PLMS index between the patients with DLB and AD ($p = 0.025$). To discriminate DLB patients from AD patients using the PLMS index, the most favorable diagnostic threshold was found to be 8.0 (AUC = 0.926). This threshold had a sensitivity of 100% and a specificity of 75.0%. A PLMS index of more than 15.0 had a sensitivity of 88.9% and a specificity of 83.3%.

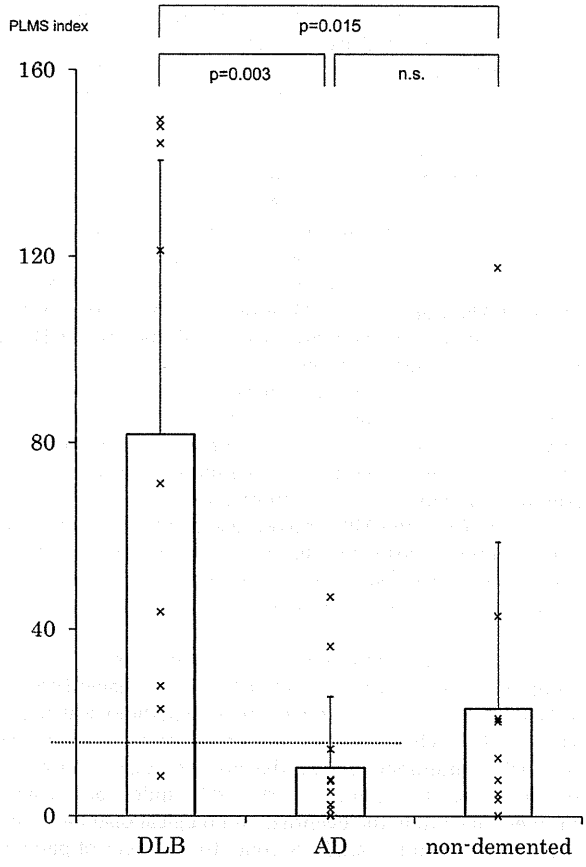

Fig. 1. Individual values for the periodic limb movements during sleep (PLMS) index in DLB patients, AD patients and non-demented patients. The boxes indicate mean and the vertical bars represent standard deviation; DLB = 81.8 ± 58.8, AD = 10.3 ± 15.3, non-demented = 23.0 ± 35.7. Mann–Whitney *U* test for multiple comparisons with the *p* values being corrected according to the Bonferroni method; significant differences in DLB vs AD ($p = 0.003$) and DLB vs Control ($p = 0.015$). The dashed line indicates the diagnostic threshold of the PLMS index of 15.0 between DLB and AD. This threshold had a sensitivity of 88.9% and a specificity of 83.3%. PLMS = periodic limb movements during sleep; AD = Alzheimer's disease; DLB = dementia with Lewy bodies; n.s. = not significant.

4. Discussion

In this study, we first observed that patients with DLB exhibited a significantly higher PLMS index compared to patients with AD.

Although the pathophysiology of PLM is not well understood, a decrease in dopaminergic activity is reported to be associated with PLM (Wetter et al., 2000; Desseilles et al., 2008; Staedt et al., 1995; Hening et al., 2004). Because abnormalities of the nigrostriatal dopaminergic pathway are also present in DLB patients, they would also be expected to exhibit a high frequency of PLM as a result of the decrease in dopaminergic activity (Walker et al., 2007; Walker and Walker, 2009).

Table 2
Sleep measures and respiratory measures of DLB patients, AD patients and non-demented patients.

Polysomnography	DLB patients	AD patients	Non-demented	*p* value
Total sleep time (min)	283.3 ± 105.8	360.3 ± 89.1	341.8 ± 70.5	n.s.
Stage N1 (%TST)	40.6 ± 12.6	29.9 ± 13.4	29.6 ± 16.5	n.s.
Stage N2 (%TST)	41.0 ± 9.4	50.5 ± 9.5	47.8 ± 12.8	n.s.
Stage N3 (%TST)	3.6 ± 4.9	6.5 ± 4.8	7.4 ± 6.1	n.s.
REM (%TST)	14.8 ± 10.2	13.1 ± 7.8	15.3 ± 8.4	n.s.
Sleep efficiency (%)	75.5 ± 14.3	76.3 ± 8.6	76.5 ± 12.5	n.s.
Sleep onset latency (min)	25.9 ± 23.9	22.2 ± 25.8	21.8 ± 16.5	n.s.
Wake time (min)	96.8 ± 74.4	112.2 ± 44.1	104.1 ± 53.0	n.s.
AHI	11.1 ± 10.5	15.0 ± 12.8	13.8 ± 14.8	n.s.
3%ODI	11.0 ± 11.1	15.2 ± 14.6	13.4 ± 14.3	n.s.
RBD (No. of patients)	4	0	0	0.004*

Values expressed as (mean ± standard deviation). * = Significant differences with the χ^2 test ($p = 0.004$). AD = Alzheimer's disease; DLB = Dementia with Lewy bodies; TST = Total sleep time; REM = Rapid eye movement; AHI = apneas hypopneas index; ODI = oxygen desaturation index; RBD = REM sleep behavior disorder; n.s. = not significant.

We also found a high prevalence of RBD in patients with DLB, as indicated previously (McKeith et al., 2005; Boeve et al., 2001, 2003). RBD is now recognized to be a manifestation of various alpha-synucleinopathies, including DLB (Boeve et al., 2007; Claassen et al., 2010), and is also frequently complicated with an increase in PLM (Fantini et al., 2002; Manconi et al., 2007). These findings suggest the presence of strong pathophysiological associations among the DLB, PD, RBD and PLM through a common central nervous system degenerative process.

Several studies have showed an increase in the PLM frequency with advancing age (Coleman et al., 1981; Ancoli-Israel et al., 1991). Bliwise et al. reported a mean PLMS index during sleep of 20.6 in elderly individuals (Bilwise et al., 1988), which was compatible with our findings in the non-demented group. The clinical use of the PLMS index as a biomarker has not been anticipated, perhaps because of the high frequency of PLM in the elderly. However, our findings indicated that the PLMS index of the DLB patients was still higher than that of elderly patients without dementia, and

furthermore, the distribution of the PLMS index was more clearly separated between the DLB patients and AD patients, likely because the non-specific variability of the PLM frequency would be overcome by the effects of predominantly progressing specific neurodegeneration in these patients.

In this study, we also compared the PLMS index between the AD group and non-demented group. No significant differences were found, but the PLMS index in the AD patients tended to be lower than that in the non-demented group. These findings might also be a characteristic feature of AD, otherwise it can not be ruled out whether the small sample size may account for a random bias with quite low PLMS indices in the AD group. Therefore, the relevance and phenomenology of PLMS especially in AD, but also in DLB has to be addressed in further studies.

Currently, DLB and AD are diagnosed according to their respective clinical diagnostic criteria (McKeith et al., 2005; McKhann et al., 1984), and their differentiation are frequently difficult. Our findings suggested the usefulness of the PLMS index to discriminate patients with DLB from those with AD. While the utilization of SPECT and MIBG myocardial scintigraphy are limited to well-equipped hospitals, simplified mobile device for the measurement of PLM (Sforza et al., 2005) is expected to perform the examination for more outpatients with dementia in clinical practice.

There are several limitations to the present study. First, we included the patients with possible DLB and probable DLB in the same DLB group. And we also did not make a pathological diagnosis of DLB or AD, which remains to be reported even in MIBG myocardial scintigraphy for the diagnosis of DLB. A prospective investigation on the course of the PLM index and cognitive impairment, including the eventual pathological diagnosis, should be examined in a future study. Second, the number of patients in each group was relatively small. However, our data indicate that there is a significant correlation between DLB and PLMS, and the data may provide a first hint for a difference between AD and DLB on the PLMS index. Third, the data for this study did not include objective or subjective measures of daytime sleepiness or day–night schedule. In the future study, an additional investigation involving a larger number of subjects should be performed.

In conclusion, we found that DLB patients exhibit a higher PLMS index than AD patients, and this index may be clinically useful in the diagnostic differentiation of DLB from AD.

Role of funding source

The funding source had no involvement in the study, design, analysis, interpretation or decision to submit this work.

Contributors

Shinichiro Hibi was involved in design, analysis, interpretation, and drafting of article. Yasuhiro Yamaguchi was responsible for conception, design, analysis, interpretation, and drafting of article. Yumi Umeda-Kameyama and Katsuya Iijima were involved in design. Toshimitsu Momose was involved in analysis. Hiroshi Yamamoto, Masahiro Akishita, and Yasuyoshi Ouchi were involved in design and interpretation. All authors had full access to the data and take responsibility for its integrity and the accuracy of the analysis.

Conflict of interest

All authors declare that they have no conflicts of interest.

Acknowledgment

This work was supported by grants-in-aid for young scientists and scientific research from the Ministry of Education, Science, Sports and Culture of Japan, and Research Grants from the Mitsui Sumitomo Insurance Welfare Foundation. We thank all participants.

References

Allen RP, Picchietti D, Hening WA, Trenkwalder C, Walters AS, Montplaisi J. Restless legs syndrome: diagnostic criteria, special considerations, and epidemiology. A report from the restless legs syndrome diagnosis and epidemiology workshop at the National Institutes of Health. Sleep Medicine 2003;4:101–19.

Ancoli-Israel S, Kripke DF, Klauber MR, Mason WJ, Fell R, Kaplan O. Periodic limb movements in sleep in community-dwelling elderly. Sleep 1991;14:496–500.

Bliwise DL, Carskadon MA, Dement WC. Nightly variation of periodic leg movements in sleep in middle aged and elderly individuals. Archives of Gerontology and Geriatrics 1988;7:273–9.

Boeve BF, Silber MH, Ferman TJ, Lucas JA, Parisi JE. Association of REM sleep behavior disorder and neurodegenerative disease may reflect an underlying synucleinopathy. Movement Disorders 2001;16:622–30.

Boeve BF, Silber MH, Parisi JE, Dickson DW, Ferman TJ, Benarroch EE, et al. Synucleinopathy pathology and REM sleep behavior disorder plus dementia or parkinsonism. Neurology 2003;61:40–5.

Boeve BF, Silber MH, Saper CB, Ferman TJ, Dickson DW, Parisi JE, et al. Pathophysiology of REM sleep behaviour disorder and relevance to neurodegenerative disease. Brain 2007;130:2770–88.

Claassen DO, Josephs KA, Ahlskog JE, Silber MH, Tippmann-Peikert M, Boeve BF. REM sleep behavior disorder preceding other aspects of synucleinopathies by up to half a century. Neurology 2010;75:494–9.

Coleman RM, Miles LE, Guilleminault CC, Zarcone Jr VP, van den Hoed J, Dement WC. Sleep-wake disorders in the elderly: polysomnographic analysis. Journal of the American Geriatrics Society 1981;29:289–96.

Colloby SJ, Fenwick JD, Williams ED, Paling SM, Lobotesis K, Ballard C, et al. A comparison of (99m) Tc-HMPAO SPET changes in dementia with Lewy bodies and Alzheimer's disease using statistical parametric mapping. European Journal of Nuclear Medicine and Molecular Imaging 2002;29:615–22.

Desseilles M, Dang-Vu T, Schabus M, Sterpenich V, Maquet P, Schwartz S. Neuroimaging insights into the pathophysiology of sleep disorders. Sleep 2008;31:777–94.

Fantini ML, Michaud M, Gosselin N, Lavigne G, Montplaisir J. Periodic leg movements in REM sleep behavior disorder and related autonomic and EEG activation. Neurology 2002;59:1889–94.

Gagnon JF, Postuma RB, Mazza S, Doyon J, Montplaisir J. Rapid-eye-movement sleep behaviour disorder and neurodegenerative diseases. Lancet Neurology 2006;5:424–32.

Hanyu H, Shimizu S, Hirao K, Kanetaka H, Iwamoto T, Chikamori T, et al. Comparative value of brain perfusion SPECT and [(123)I]MIBG myocardial scintigraphy in distinguishing between dementia with Lewy bodies and Alzheimer's disease. European Journal of Nuclear Medicine and Molecular Imaging 2006;33:248–53.

Hening WA, Allen RP, Earley CJ, Picchietti DL, Silber MH. Restless legs syndrome task force of the standards of practice committee of the American academy of sleep medicine. An update on the dopaminergic treatment of restless legs syndrome and periodic limb movement disorder. Sleep 2004;27:560–83.

Iber C, Ancoli-Israel S, Chesson A, Quan S, for the American Academy of Sleep Medicine. The AASM manual for the scoring of sleep and associated events; rules, terminology and technical specifications. 1st ed. Westchester, IL: American Academy of Sleep Medicine; 2007.

Lavault S, Bloch F, Houeto JL, Konofal E, Welter ML, Agid Y, et al. Periodic leg movements and REM sleep without atonia in Parkinson's disease with camptocormia. Movement Disorders 2009;24:2419–23.

Lobotesis K, Fenwick JD, Phipps A, Ryman A, Swann A, Ballard C, et al. Occipital hypoperfusion on SPECT in dementia with Lewy bodies but not AD. Neurology 2001;56:643–9.

Manconi M, Ferri R, Zucconi M, Fantini ML, Plazzi G, Ferini-Strambi L. Time structure analysis of leg movements during sleep in REM sleep behavior disorder. Sleep 2007;30:1779–85.

McKeith IG, Galasko D, Kosaka K, Perry EK, Dickson DW, Hansen LA, et al. Consensus guidelines for the clinical and pathologic diagnosis of dementia with Lewy bodies: report of the consortium on DLB international workshop. Neurology 1996;47:1113–24.

McKeith IG, Dickson DW, Lowe J, Emre M, O'Brien JT, Feldman H, et al. Diagnosis and management of dementia with Lewy bodies: third report of the DLB consortium. Neurology 2005;65:1863–72.

McKhann G, Drachman D, Folstein M, Katzman R, Price D, Stadlan EM. Clinical diagnosis of Alzheimer's disease: report of the NINCDS-ADRDA Work Group under the auspices of Department of Health and Human Services Task Force on Alzheimer's Disease. Neurology 1984;34:939–44.

Rose KM, Beck C, Tsai PF, Liem PH, Davila DG, Kleban M, et al. Sleep disturbances and nocturnal agitation behaviors in older adults with dementia. Sleep 2011;34:779–86.

Sforza E, Johannes M, Claudio B. The PAM-RL ambulatory device for detection of periodic leg movements: a validation study. Sleep Medicine 2005;6:407–13.

Staedt J, Stoppe G, Kogler A, Riemann H, Hajak G, Munz DL, et al. Nocturnal myoclonus syndrome (periodic movements in sleep) related to central dopamine D2-receptor alteration. European Archives of Psychiatry and Clinical Neuroscience 1995;245:8–10.

Walker RW, Walker Z. Dopamine transporter single photon emission computerized tomography in the diagnosis of dementia with Lewy bodies. Movement Disorders 2009;24:S754–9.

Walker Z, Jaros E, Walker RW, Lee L, Costa DC, Livingston G, et al. Dementia with Lewy bodies: a comparison of clinical diagnosis, FP-CIT single photon emission computed tomography imaging and autopsy. Journal of Neurology, Neurosurgery and Psychiatry 2007;78:1176–81.

Wetter TC, Collado-Seidel V, Pollmächer T, Yassouridis A, Trenkwalder C. Sleep and periodic leg movement patterns in drug-free patients with Parkinson's disease and multiple system atrophy. Sleep 2000;23:361–7.

Yoshita M, Taki J, Yamada M. A clinical role for [(123)I]MIBG myocardial scintigraphy in the distinction between dementia of the Alzheimer's-type and dementia with Lewy bodies. Journal of Neurology, Neurosurgery and Psychiatry 2001;71:583–8.

Zucconi M, Ferri R, Allen R, Baier PC, Bruni O, Chokroverty S, et al. The official World Association of Sleep Medicine (WASM) standards for recording and scoring periodic leg movements in sleep (PLMS) and wakefulness (PLMW) developed in collaboration with a task force from the International Restless Legs Syndrome Study Group (IRLSSG). Sleep Medicine 2006;7:175–83.

Ann Nucl Med (2012) 26:698–706
DOI 10.1007/s12149-012-0629-9

ORIGINAL ARTICLE

Voxel-based comparison of preoperative FDG-PET between mesial temporal lobe epilepsy patients with and without postoperative seizure-free outcomes

Miwako Takahashi · Tsutomu Soma · Kensuke Kawai · Keitraro Koyama · Kuni Ohtomo · Toshimitsu Momose

Received: 21 May 2012 / Accepted: 24 June 2012 / Published online: 19 July 2012

Abstract
Objective This study aims to elucidate differences in preoperative cerebral glucose metabolism between patients who did and did not become seizure free after unilateral mesial temporal lobe epilepsy (mTLE) surgery. We hypothesized that regional glucose metabolism on preoperative fluorodeoxyglucose positron emission tomography (FDG-PET) in patients with seizure-free outcomes differed from that in patients who were not seizure free after appropriate epilepsy surgery for unilateral mTLE. In this study, we compared preoperative FDG-PET findings between these two patient groups by applying a statistical analysis approach, with a voxel-based Asymmetry index (AI), to improve sensitivity for the detection of hypometabolism.
Methods FDG-PET scans of 28 patients with medically refractory mTLE, of whom 17 achieved a seizure-free outcome (Engel class 1 a–b) during a postoperative follow-up period of at least 2 years, were analyzed retrospectively. Voxel values were adjusted by the AI method as well as the global normalization (GN) method. Two types of statistical analysis were performed. One was a voxel severity analysis with comparison of voxel values at the same coordinate, and the other was extent analysis with comparison of the number of significant voxels in the anatomical areas predefined with Talairach's atlas.
Results In the voxel severity analysis, significant hypometabolism restricted to the ipsilateral temporal tip and hippocampal area was detected in the postoperative seizure-free outcome group as compared to controls. No significant area was detected in the non-seizure-free group as compared to controls (family-wise error corrected, $p < 0.05$). With extent analysis using a low threshold, the extents of hypometabolism in the ipsilateral hippocampal, frontal and thalamic areas were larger in the seizure-free than in the non-seizure-free group ($p = 0.01$, 0.03 and 0.01, respectively.) On the other hand, in the contralateral frontal and thalamic areas, extents of hypometabolism were smaller in the seizure-free than in the non-seizure-free group ($p = 0.01$ and 0.01).
Conclusions We found the preoperative distribution of hypometabolism to differ between the two patient groups. Severe hypometabolism restricted to the unilateral temporal lobe, with ipsilateral dominant hypometabolism including mild decreases, may support the existence of an epileptogenic focus in the unilateral temporal lobe and a favorable seizure outcome after mTLE surgery.

Keywords Asymmetry index · FDG-PET · Mesial temporal lobe epilepsy · Postoperative outcome

M. Takahashi · T. Soma · K. Koyama · K. Ohtomo · T. Momose (✉)
Department of Radiology, Graduate School of Medicine, University of Tokyo, 3-1, Hongo 7-Chome, Bunkyo-ku, Tokyo 113-8655, Japan
e-mail: tmomo-tky@umin.ac.jp

T. Soma
Software Development Group, Product Management and Marketing Department, FUJIFILM RI Pharma Co., Ltd, Tokyo, Japan

K. Kawai
Department of Neurosurgery, Graduate School of Medicine, University of Tokyo, Tokyo, Japan

Introduction

Epilepsy surgery is an important treatment for patients with medically refractory epilepsy. Surgery for temporal lobe